

## The effect of carrier mobility in organic solar cells

Ji-Ting Shieh, Chiou-Hua Liu, Hsin-Fei Meng, Shin-Rong Tseng, Yu-Chiang Chao, and Sheng-Fu Horng

Citation: *Journal of Applied Physics* **107**, 084503 (2010); doi: 10.1063/1.3327210

View online: <http://dx.doi.org/10.1063/1.3327210>

View Table of Contents: <http://scitation.aip.org/content/aip/journal/jap/107/8?ver=pdfcov>

Published by the [AIP Publishing](#)

---

### Articles you may be interested in

[Improving the efficiency of an organic solar cell by a polymer additive to optimize the charge carriers mobility](#)  
*Appl. Phys. Lett.* **99**, 223305 (2011); 10.1063/1.3664127

[Imbalanced mobilities causing S-shaped IV curves in planar heterojunction organic solar cells](#)  
*Appl. Phys. Lett.* **98**, 063301 (2011); 10.1063/1.3553764

[Nanosecond response of organic solar cells and photodetectors](#)  
*J. Appl. Phys.* **105**, 104513 (2009); 10.1063/1.3130399

[Relation between carrier mobility and cell performance in bulk heterojunction solar cells consisting of soluble polythiophene and fullerene derivatives](#)  
*Appl. Phys. Lett.* **87**, 132105 (2005); 10.1063/1.2058210

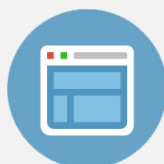
[The roles of injection and mobility in organic light emitting diodes](#)  
*J. Appl. Phys.* **83**, 5399 (1998); 10.1063/1.367369

---



## Re-register for Table of Content Alerts

Create a profile.



Sign up today!



## The effect of carrier mobility in organic solar cells

Ji-Ting Shieh,<sup>1</sup> Chiou-Hua Liu,<sup>2</sup> Hsin-Fei Meng,<sup>3,a)</sup> Shin-Rong Tseng,<sup>3</sup> Yu-Chiang Chao,<sup>3</sup> and Sheng-Fu Horng<sup>2</sup>

<sup>1</sup>*Institute of Photonics Technologies, National Tsing Hua University, Hsinchu 300, Taiwan, Republic of China*

<sup>2</sup>*Institute of Electronics Engineering, National Tsing Hua University, Hsinchu 300, Taiwan, Republic of China*

<sup>3</sup>*Institute of Physics, National Chiao Tung University, Hsinchu 300, Taiwan, Republic of China*

(Received 24 November 2009; accepted 21 January 2010; published online 21 April 2010)

The microscopic states and performance of organic solar cell are investigated theoretically to explore the effect of the carrier mobility. With Ohmic contacts between the semiconductor and the metal electrodes there are two origins of carriers in the semiconductor: the photocarriers generated by photon absorption and the dark carriers diffused from the electrodes. The power efficiency of the solar cell is limited by the recombination of a carrier with either the photocarrier or a dark carrier. Near the short-circuit condition the photocarrier recombination in the semiconductor bulk decreases as the mobility increases. Near the open-circuit condition the dark carrier recombination increases with the mobility. These two opposite effects balance with one another, resulting in an optimal mobility about  $10^{-2}$  cm<sup>2</sup>/V s which gives the highest power conversion efficiency. The balance of the electron and hole mobilities are not necessary to maintain the optimal efficiency also because of the balance of the photocarrier and dark carrier recombination. The efficiency remains about the same as one carrier mobility is fixed at  $10^{-2}$  cm<sup>2</sup>/V s while the other one varies from  $10^{-1}$  to  $10^{-3}$  cm<sup>2</sup>/V s. For solar cell with a Schottky barrier between the semiconductor and the metal electrode there is no dark carrier recombination. The efficiency therefore always increases with the mobility. © 2010 American Institute of Physics. [doi:10.1063/1.3327210]

### I. INTRODUCTION

Organic solar cells have attracted great attention recently because of their unique properties such as the potential for high efficiency, easy solution process for low cost fabrication, and the application for the flexible devices. Bulk heterojunctions (BHJs) of organic solar cells use the mixture of donor and acceptor components in the bulk so that the process of exciton diffusion to the charge separation donor-acceptor interface is efficient. The power conversion efficiency (PCE) exceeding 5% of organic BHJ solar cell has been reported.<sup>1,2</sup> Much effort in experiments have been made to improve the performance of the device recently, but the efficiency remains around 5%.<sup>3-6</sup> Obviously there remain many fundamental questions regarding to the origins of efficiency limitation and the device concept to raise the performance. In addition, theoretical methods are established to understand the physical process of the BHJ solar cell more clearly. There are four processes that contribute to the efficiency of the organic BHJ solar cell, including the absorption of photons and the creation of excitons, exciton diffusion to the charge separation interface, exciton dissociation to free electron and hole by the heterojunctions, and carrier transport and collection by the electrodes.<sup>7</sup> Among the factors, the photon absorption reaches 90% with the thickness of the active layer larger than 200 nm,<sup>1</sup> and the exciton dissociation can be very efficient due to the large amounts of charge separation interfaces in the BHJ solar cells. The key factor to

decide the efficiency is the process of carriers transport and collection by the electrodes. Therefore the carrier mobility is a critical factor to determine the efficiency. Some theoretical models are established for the organic solar cell. The optimal mobility on organic solar cell was discussed in previous works.<sup>8-11</sup> The notion of quasi-Fermi level was introduced and the difference between the electron and hole Fermi levels was shown to decrease as the mobility increases.<sup>8</sup> The quasi-Fermi level is however just another expression of the open-circuit voltage, and there were no studies on what happens to the carrier density and recombination profile with increasing mobility. The exciton dissociation rate into free electron-hole pair was shown to be limited by geminate recombination<sup>9,12</sup> and depends on the mobility. Such mobility-dependent dissociation was incorporated into the device model.<sup>10</sup> The exciton dissociation rate is however near unity for mobility over  $10^{-3}$  cm<sup>2</sup>/V s,<sup>8</sup> so this effect is expected to play a minor role for high mobility. Surface recombination was raised as one possibility for efficiency reduction at high mobility.<sup>11</sup> Such model requires a surface recombination velocity as an extra parameter whose microscopic origin is not clear. In addition, it is unlikely for the minority carrier to reach the electrode interface because of the strong recombination with the majority carrier near the interface, as discussed below. A distribution in the binding energy of charge-transfer state, as a precursor to free electron-hole pair, was considered as a possible source of mobility dependence of efficiency.<sup>11</sup> The energy of the charge-transfer state is determined by the energy levels of donor and acceptor. There would be a wide range of such energy only when there was a

<sup>a)</sup>Author to whom correspondence should be addressed. Electronic mail: meng@mail.nctu.edu.tw.

mixture of materials. The mobility-dependent transfer among the charge-transfer state is therefore not expected to have a major effect on the solar cell with a single donor and a single acceptor material.

It is expected that the majority of the effects of the mobility is not derived from the secondary factors such as exciton dissociation and surface recombination but lie within the essential model with only drift-diffusion current, unit exciton dissociation probability, and Langevin recombination.<sup>9,13</sup> Recombination is known to be the dominant factor to limit the efficiency and the effect of mobility should enter through recombination. It is clear that recombination increases in the low mobility limit because of the photocarrier accumulation inside the bulk. What happens to the recombination in the high mobility limit is however less known. There is so far no clear and complete understanding of the effect of mobility on the recombination and more generally microscopic physical state of the solar cell and the overall conversion efficiency. It is generally believed that the improvement of the efficiency requires a high mobility because of an easier photocarrier extraction. However it is not known whether there exist an optimal mobility at which the efficiency reaches a maximum within the essential model. In this work we employ a microscopic numerical model for a comprehensive study on the effect of carrier mobility on the recombination of organic solar cell. The distributions of carrier density, recombination rate, and electric field are calculated as functions of the mobility for various voltages. Both the cases of symmetrical electron-hole mobility and the un-symmetrical mobilities are considered. The energy barrier height between the semiconductor and the metal electrodes is varied.

Once an electron-hole pair is created by photon absorption, there are three possible final destinations for the electron. It can either be collected by the low work function cathode, or recombine with a hole, or collected by the high work function anode. Below we will name the cathode as the right electrode for the electron and anode the wrong electrode. The destinations for the hole are similar. Only the electrons collected by the right electrode contribute to the desired photocurrent for power conversion. In our calculation for Ohmic contact the wrong electrode collection is negligible so the most important limit for the solar cell efficiency is the carrier recombination. For an electron it can recombine with holes from two origins, one is the photogeneration and another is the diffusion from the high work function anode. The carriers which come from the electrode diffusion are called dark carriers because they are present even without illumination. The total recombination can therefore be viewed as a combination of photocarrier recombination and dark carrier recombination. Near the short-circuit condition the high built-in electric field prevents the dark carriers from entering the bulk of the semiconductor so the dark carriers concentrate around the semiconductor metal interface. On the other hand near the open-circuit condition there is almost a flat energy band so the dark carriers easily penetrate inside the bulk. Interestingly the photocarrier recombination and dark carrier recombination have opposite dependence on the carrier mobility. At low mobility the pho-

tocarriers accumulate inside the bulk and its density is high resulting in high recombination. At high mobility the dark carrier diffusion from the metal to the semiconductor becomes rapid resulting in high dark carrier recombination. Our calculation shows that at low voltage the photocurrent is lower for low mobility case because of strong photocarrier recombination, while the open-circuit voltage  $V_{OC}$  is lower for high mobility case because of the predominant dark carrier recombination. The two opposite effects of the mobility give an optimal mobility where the efficiency reaches a maximal, in contrast to the general concept that the increase in mobility is also beneficial for the solar cell.

The behaviors of the solar cell change dramatically as the Ohmic contact is replaced by a Schottky contact with large energy barrier. Our calculation shows that there are no longer dark carriers because of the energy barrier so the recombination is dominated by the photocarrier recombination. The solar cell efficiency then monotonically increases with the carrier mobility because of the rapid motion toward the electrodes under built-in field. Furthermore the collection by the wrong electrode becomes important with Schottky contact. Indeed with Ohmic contact it is difficult for an electron to reach the high work function anode because of the high density of holes around the interface, so recombination will occur before reaching the interface. However for Schottky contact there is no such hole layer near the anode so the electrons can reach both sides, especially near the open-circuit condition where the band is nearly flat and the carrier motions are driven by diffusion rather than electric field. Even though Ohmic contact is always preferred in practice because of the optimal open-circuit voltage, the theoretical comparison with the Schottky contact provides a great insight on the origins of effect of carrier mobility on the recombination processes and the overall efficiency.

## II. MODEL AND EQUATION

In this work we calculate the distributions of the carrier density, recombination, electron and hole current density, and potential energy in the device to investigate the effect of carrier mobility. The current voltage relation under solar illumination gives the fill factor (FF), PCE, short-circuit current ( $J_{SC}$ ), and open-circuit voltage ( $V_{OC}$ ). By deriving the continuity equation at steady state the total current density  $J_t$  is expressed as

$$-\frac{dJ_n}{qdx} = G - R, \quad (1)$$

$$J_n(0) - J_n(L) = \int (qG - qR)dx, \quad (2)$$

$$J_n(0) - J_n(L) = J_g - J_r. \quad (3)$$

The same reason

$$J_p(L) - J_p(0) = J_g - J_r. \quad (4)$$

The definition of total current is given by

$$J_t = -[J_n(0) + J_p(0)] = -[J_n(L) + J_p(L)], \quad (5)$$

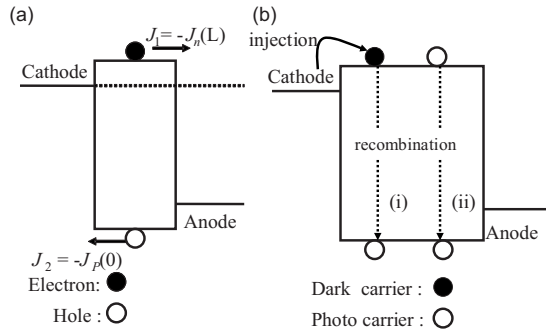


FIG. 1. (a) Schematic diagram of the carriers collected by the wrong electrodes.  $J_1$  ( $J_2$ ) is the electrical current of electron (hole) collected by the anode (cathode). (b) Recombination paths for photocarriers in the active layer. Path (i) is the recombination between dark carriers and photocarriers. Path (ii) is the recombination among photocarriers themselves.

$$J_t - J_r = -J_n(0) - J_p(0) - J_r. \quad (6)$$

Substitution Eq. (3) into Eq. (6)

$$J_t - J_r = -J_n(L) - J_p(0) - J_g, \quad (7)$$

$$J_t - J_r = J_1 + J_2 - J_g, \quad (8)$$

$$J_t = J_1 + J_2 - J_g + J_r, \quad (9)$$

where  $J_1$  ( $J_2$ ) is the electrical current density of electrons (holes) entering the anode (cathode) as shown in Fig. 1(a),  $J_g$  is photogeneration current density, and  $J_r$  is the recombination current density resulted from dark carrier recombination and photocarrier recombination as shown in Fig. 1(b).  $G$  is the photocarrier generation rate by sunlight, which is taken constant with respect to the position for simplicity. The recombination rate  $R$  has a bimolecular form  $R = \gamma np$  with the Langenvin recombination coefficient  $\gamma$  given by<sup>14,15</sup>

$$\gamma = \frac{4\pi e}{\epsilon} (\mu_n + \mu_p). \quad (10)$$

The dark carriers are the carriers diffused from the metal to the semiconductor. Dark carrier recombination means the dark carriers recombine with the photocarriers. The positive electrical current is defined to be the one flowing to the left side in Fig. 1(a). In solar cell the electrical current flows to the right so it is negative in our calculations below. Both  $J_g$  and  $J_r$  are positive by definition.  $J_1$  and  $J_2$  are also both positive because at the wrong interface the carriers can only leave the semiconductor because of the extremely large injection barriers from the metal side. The generation current is therefore compromised by the three terms in Eq. (9), resulting from the carrier recombination, and electron entering the anode, and the hole entering the cathode.  $J_1$ ,  $J_2$ , and  $J_r$  are mobility dependent.

The theoretical model is based on the previous works on organic light-emitting diodes.<sup>16,17</sup> We choose physical parameters from the system of poly(3-hexylthiophene-2,5-diyl) (P3HT) donor and (6,6)-phenyl C61 butyric acid methyl ester (PCBM) acceptor blend, and the electron affinity of PCBM is 3.7 eV and the ionization potential of P3HT is 5.1 eV. All values of the physical variables in the thermal equilibrium can be solved by equilibrium carrier density expres-

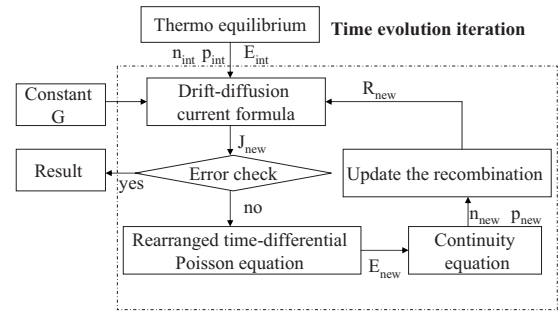


FIG. 2. Flow diagram of the simulation program. At first, the thermal equilibrium solution is solved to get the initial condition in time evolution. Then, the bias voltage is applied within a pseudotime so that the steady state is reached. The steady state is treated by solving the continuity equation coupled with drift-diffusion current relations and Poisson's equation iteratively.

sion coupled with Poisson's equation. The thermal equilibrium is taken as the initial condition for the time evolution to state under illumination and applied voltage. The equilibrium equations are given as following:

$$n = n_0 e^{\{-[E_c - e\varphi(x) - E_F]\}/\beta}, \quad (11)$$

$$p = n_0 e^{\{-[E_v - e\varphi(x) - E_F]\}/\beta}, \quad (12)$$

$$\frac{\partial^2 \varphi(x)}{\partial x^2} = -\frac{q(p - n)}{\epsilon}, \quad (13)$$

where  $\beta = 1/kT$ ,  $n_0$  is the density of state of the semiconductor,  $E_c$  is the energy of the band conduction band,  $E_v$  is the energy of the valance band,  $\varphi(x)$  is electric potential,  $x$  is the position coordinate,  $E_F$  is the Fermi level,  $\epsilon$  is the semiconductor dielectric constant, and  $q$  is the absolute value of electron charge. The bias voltage is applied within a voltage ramp and the system reaches the steady state afterwards. The steady state is treated by solving iteratively the continuity Eqs. (14) and (15) and Poisson's Eq. (13). As shown in Eqs. (16) and (17), the currents are combination of drift and diffusion terms current relations and Poisson's equation

$$\frac{\partial n}{\partial t} = \frac{1}{q} \left( \frac{\partial J_n}{\partial x} \right) + G - R, \quad (14)$$

$$\frac{\partial p}{\partial t} = \frac{-1}{q} \left( \frac{\partial J_p}{\partial x} \right) + G - R, \quad (15)$$

$$J_n = q\mu \left( nE + \frac{kT}{q} \frac{\partial n}{\partial x} \right), \quad (16)$$

$$J_p = q\mu \left( nE - \frac{kT}{q} \frac{\partial p}{\partial x} \right). \quad (17)$$

$J_n$  and  $J_p$  are the electron and hole current densities, respectively. The mobility  $\mu$  is assumed to be field independent and symmetrical for electron and hole initially. The flow chart of simulation program is shown in Fig. 2. The boundary condition is determined by the carrier injection at the contact. The total hole electrical current density  $J_p$  is given by<sup>18</sup>

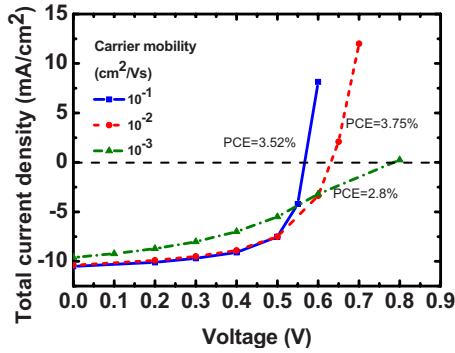


FIG. 3. (Color online) The calculation of total current density as a function of applied voltage with thickness of 230 nm and barrier height 0.2 eV for various mobilities.

$$J_t(x) = J_{\text{device}} = J_{\text{th}} - J_{\text{ir}}, \quad (18)$$

Where  $J_{\text{th}}$  is thermionic emission current given by

$$J_{\text{th}} = AT^2 \exp\left(-\frac{\phi_B}{kT}\right). \quad (19)$$

$A$  is the Richardson constant,  $\phi_B = \phi_{B0} - \sqrt{q||E||/4\pi\epsilon}$  is the Schottky barrier height including image force barrier lowering. The interface recombination current is proportional to the carrier density at the contact, and is given by

$$J_{\text{ir}} = \nu p(x), \quad (20)$$

where  $\nu$  can be determined by balance of thermionic emission current and interface recombination current in thermal equilibrium, with the result  $\nu = AT^2/n_0$ .

### III. IN OHMIC CONTACT DEVICES WITH BALANCE OF THE ELECTRON AND HOLE MOBILITIES

We first apply the model to the case of low barrier height between the metal Fermi level and the semiconductor energy bands i.e., the Ohmic contact. The barrier height of carrier injection is chosen to be 0.2 eV and symmetric on both sides. The lowest unoccupied molecular orbital (LUMO) of the semiconductor and the highest occupied molecular orbital (HOMO) of semiconductor act as valence and conduction band of the semiconductor to describe the blend of donor and acceptor. The conduction band is 3.7 eV, the valence band is 5.1 eV, and generation  $G$  is  $3.145 \times 10^{21}$ . The  $J_t$ - $V$  relation under different carrier mobilities from  $10^{-1}$  to  $10^{-3}$  cm<sup>2</sup>/V s

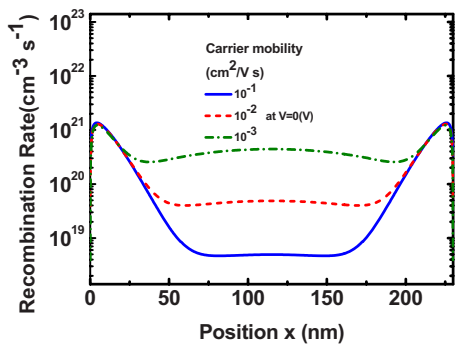


FIG. 4. (Color online) The recombination distribution for various mobilities with barrier height 0.2 eV at short-circuit condition.

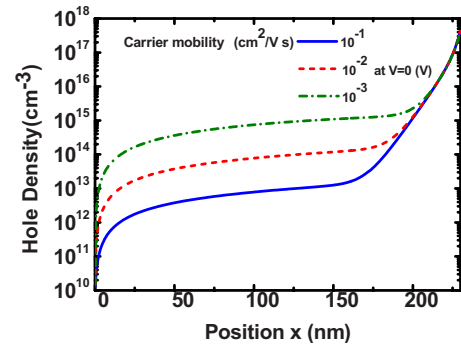


FIG. 5. (Color online) The hole density distribution for various mobilities in the bulk with barrier height 0.2 eV at short-circuit condition.

is shown in Fig. 3.  $V_{\text{OC}}$  is the voltage with zero current. It decreases dramatically as the mobility increases, resulting from the serious dark carrier recombination when carrier mobility is high.<sup>13</sup> It shows different behaviors between short-circuit condition at 0 V and flat band condition about 0.6 V. At the short-circuit condition the recombination occurs mostly near semiconductor and electrode interface and there is less recombination in the bulk, shown in Fig. 4. The recombination near the electrode can be regarded as dark carrier recombination. The strong built-in voltage in short-circuit condition prevents the dark carriers from diffusing deeply to the bulk as shown in Figs. 5 and 6. Away from the recombination in the bulk can be regarded as photocarrier recombination. When carrier mobility increases the photocarriers recombination in the bulk reduces dramatically. Photocarriers with low mobility are difficult to transport and be collected by electrodes. They accumulate in the bulk and recombine with other photocarriers. Nevertheless the recombination current at the short-circuit condition contributes only small loss to the total current. At flat band condition, the recombination occurs seriously not only near the electrode but also in the bulk, as shown in Fig. 7. In this condition the photocarrier recombination decreases and dark carrier recombination increases as the mobility rises. The competition of the two trends leads to that both low mobility ( $10^{-3}$  cm<sup>2</sup>/V s) and high mobility ( $10^{-1}$  cm<sup>2</sup>/V s) contributes to major current loss. The calculation predicts that the carrier mobility about  $10^{-2}$  cm<sup>2</sup>/V s gives the balance and optimal device performance. Near the open-circuit condition the dark carriers diffuse easily to bulk and the dark carrier

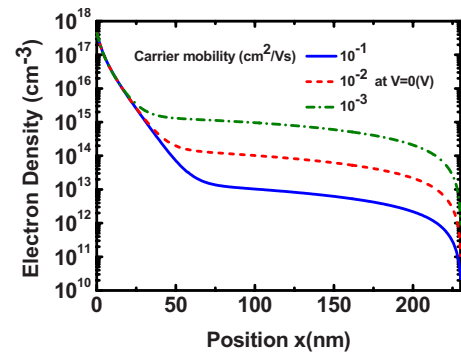


FIG. 6. (Color online) The electron density distribution for various mobilities in the bulk with barrier height 0.2 eV at short-circuit condition.

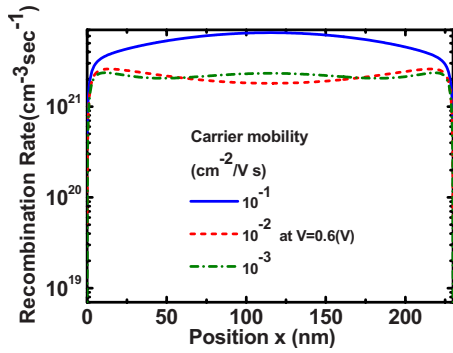


FIG. 7. (Color online) The recombination distribution for various mobilities in the bulk with barrier height 0.2 eV at flat band condition.

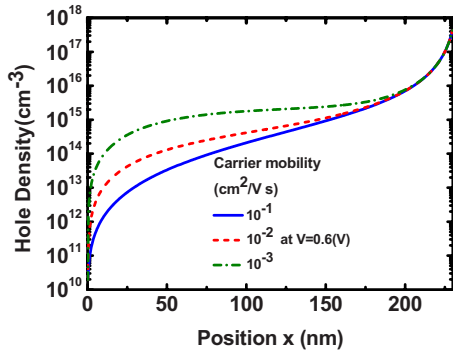


FIG. 8. (Color online) The hole density distribution for various mobilities in the bulk with barrier height 0.2 eV at flat band condition.

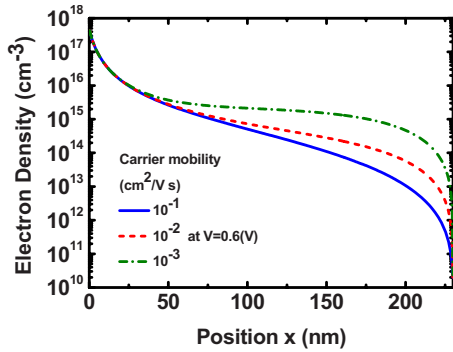


FIG. 9. (Color online) The electron density distribution for various mobilities in the bulk with barrier height 0.2 eV at flat band condition.

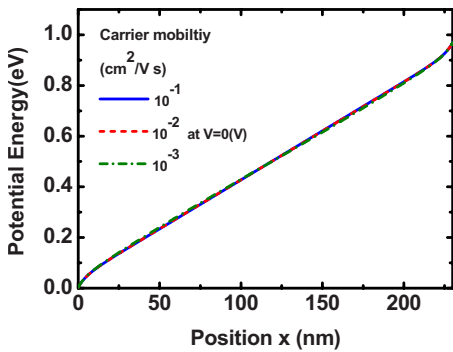


FIG. 10. (Color online) The potential energy distribution for various mobilities in the bulk with barrier height 0.2 eV at short-circuit condition.

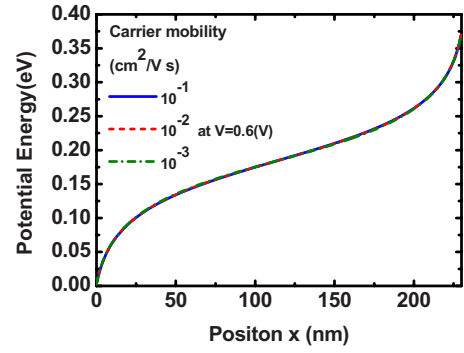


FIG. 11. (Color online) The potential energy distribution for various mobilities in the bulk with barrier height 0.2 eV at flat band condition.

density is higher than the short-circuit condition, as shown in Figs. 8 and 9. Figures 10 and 11 show the potential energy profiles of the short-circuit condition and flat band condition. The diffusion of dark carriers creates the band bending which is stronger near  $V_{OC}$ . The potential profile is nearly independent on mobility.

#### IV. IN OHMIC CONTACT DEVICES WITH UNBALANCE OF THE ELECTRON AND HOLE MOBILITIES

Until now we set hole mobility to be equal to electron mobility and determine the mobility around  $10^{-2}$   $\text{cm}^2/\text{V s}$  for optimal solar cell efficiency. The optimal mobility results from the competition between the dark carrier recombination and the photocarrier recombination under the Ohmic contact condition. For more practical situation, we consider the case with distinct values of hole and electron mobility. The electron mobility is fixed to be  $10^{-2}$   $\text{cm}^2/\text{V s}$  which is the best value for symmetrical, and the hole mobility increases from  $10^{-4}$  to  $10^{-1}$   $\text{cm}^2/\text{V s}$ . The results are shown in Fig. 12 and summarized in Table I. As proportion of the hole mobility to the electron mobility from 0.1 to 10 the efficiency remains nearly the same. Fixing the hole mobility as  $10^{-2}$   $\text{cm}^2/\text{V s}$  and change electron mobility will lead to the same result because the system symmetry. Therefore we predict that the efficiency remains high if one kind of carrier mobility is about  $10^{-2}$   $\text{cm}^2/\text{V s}$  and the other is within a wide “safe” range from  $10^{-1}$  to  $10^{-3}$   $\text{cm}^2/\text{V s}$ . This is different from the common view that the electron and hole mobility should be about the same.<sup>19</sup> The preliminary experimental data of

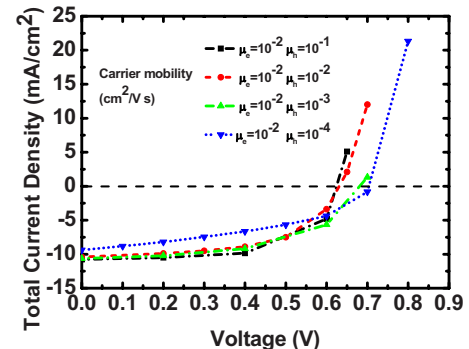


FIG. 12. (Color online) Calculated total current density as a function of applied voltage with thickness of 230 nm and barrier height 0.2 eV for unbalance of hole and electron mobility.

TABLE I. The device performance for singer layer structure with fixed electron mobility and various hole mobilities. FF is fill factor and PCE is the power conversion efficiency.

Mobility (cm <sup>2</sup> /V s)	V <sub>OC</sub> (V)	J <sub>SC</sub> (mA/cm <sup>2</sup> )	J <sub>r</sub> at V=0(V) (mA/cm <sup>2</sup> )	FF (%)	PCE (%)
μ <sub>e</sub> =10 <sup>-2</sup> μ <sub>h</sub> =10 <sup>-1</sup>	0.62	10.8	4.1 × 10 <sup>-1</sup>	58	3.93
μ <sub>e</sub> =10 <sup>-2</sup> μ <sub>h</sub> =10 <sup>-2</sup>	0.63	10.4	8.0 × 10 <sup>-1</sup>	57	3.72
μ <sub>e</sub> =10 <sup>-2</sup> μ <sub>h</sub> =10 <sup>-3</sup>	0.68	10.6	5.6 × 10 <sup>-1</sup>	51	3.73
μ <sub>e</sub> =10 <sup>-2</sup> μ <sub>h</sub> =10 <sup>-4</sup>	0.70	9.4	1.9	43	2.83

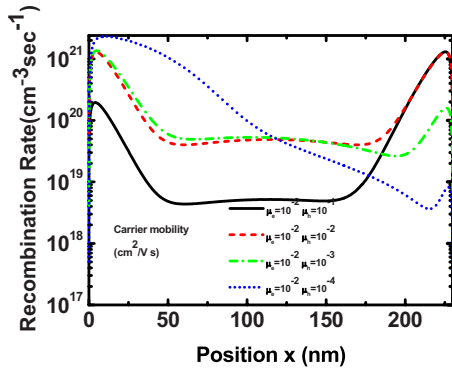


FIG. 13. (Color online) The recombination distribution with barrier height 0.2 eV for unbalance of hole and electron mobility at short-circuit condition.

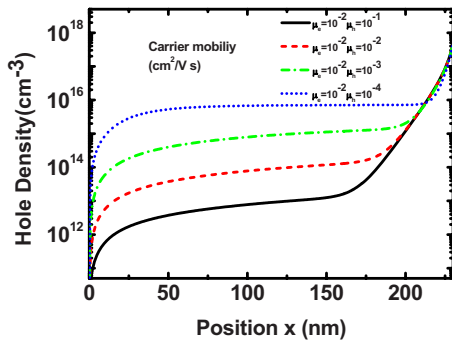


FIG. 14. (Color online) The hole density distribution with barrier height 0.2 eV for unbalance of hole and electron mobility. The bias condition is short-circuit condition.

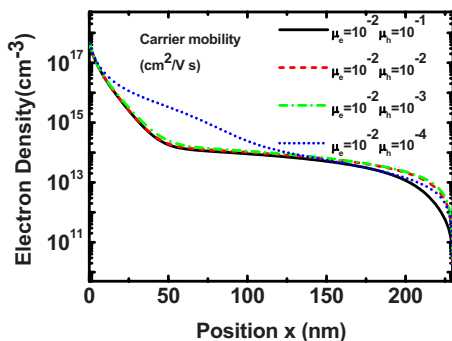


FIG. 15. (Color online) The electron density distribution with barrier height 0.2 eV for unbalance of hole and electron mobility. The bias condition is short-circuit condition.

polymer-based solar cells fabricated by high hole mobility polymers also show no superior efficiency even more work still needed to be done.<sup>20</sup> Again the high tolerance of the ratio between electron and hole mobility is due to the balance of the opposite effect of mobility on photocarrier recombination and dark carrier recombination. With unequal mobilities the recombination coefficient is

$$\gamma = \frac{q}{\epsilon} \min(\mu_n, \mu_p). \tag{21}$$

The slow carrier determines the recombination process in the bulk because the fast carrier should wait for the slow one to recombine.<sup>21</sup> Figure 13 shows the recombination rate in the bulk with different mobility ratio. If the ratio is larger than 100, it shows strong recombination in the bulk. Figure 14 shows the hole density distribution in the bulk. There is always a high hole density near anode due to the dark carrier diffusion. The hole carrier density increases in the bulk uniformly as hole mobility is decreasing because of the slow collection of the photocarrier. Figure 15 shows the electron density, the distributions are about the same when the ratios of electron and hole mobility are from 0.1 to 10. Once the hole mobility decreases to 10<sup>-4</sup> cm<sup>2</sup>/V s with mobility ratio 100, the electron density distribution becomes higher due to the attractive potential from accumulated holes in the bulk. In other words, the accumulation of slows holes will eventually holds the electrons in the bulk.

**V. IN SCHOTTKY CONTACT DEVICES**

To eliminate the effect of the dark recombination and isolate the effect of photocarrier recombination, we consider the device with Schottky contact. The J<sub>T</sub>-V relation is shown in Fig. 16 and the inset is the recombination current density

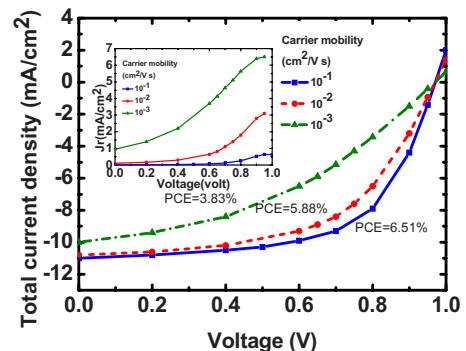


FIG. 16. (Color online) The calculation of total current density as a function of applied voltage with thickness of 230 nm and barrier height 1 eV for various mobilities. The inset shows the recombination current.

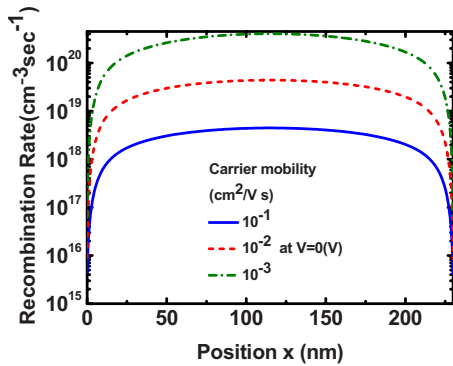


FIG. 17. (Color online) The recombination distribution for various mobilities in the bulk with Schottky contact at short-circuit condition.

$J_r$ . Unlike the Ohmic contact case the behaviors  $V_{OC}$  is about the same with various mobilities because there is no dark recombination in the Schottky contact. The total currents show different behaviors at short-circuit condition especially when the mobility is as low as ( $10^{-3}$   $\text{cm}^2/\text{V s}$ ). In this case the total current is only limited by the photocarrier recombination and the current entering the wrong electrode according to Eq. (9). The photocarrier recombination becomes strong when the mobility is low due to the photocarrier accumulation in the bulk. The generation rate  $G$  is taken to be the same as the Ohmic contact case. In Fig. 17 the distribution of carrier recombination rate is shown to be large and uniform in the bulk. The carrier recombination decreases as mobility increases. There is no dark carrier in Schottky contact therefore the recombination is not pronounced near the electrodes. For further details the distribution of the electron density  $n(x)$  and hole density  $p(x)$  are shown in Figs. 18 and 19, respectively. The electron density and hole density decrease when the carrier mobility increases. When the mobility is high, the photocarriers can easily transport and be collected by the electrodes, with little carrier accumulation in the bulk. In this case the carriers collected by the wrong electrodes, i.e.,  $J_1$  and  $J_2$  in Eq. (9) and Fig. 1(a) become important factors to decide the total current. Figure 20 shows  $J_1-V$  relation. As mobility increases  $J_1$  becomes higher near the flat band voltage.  $J_1$  always nearly zero at short-circuit voltage because the built-in voltage prevents the carriers from collection by the wrong electrodes. The value of  $J_1$  and  $J_2$  under different mobilities and positions are summarized in Table II. The values of  $J_1$  and  $J_2$  are almost one-third of the

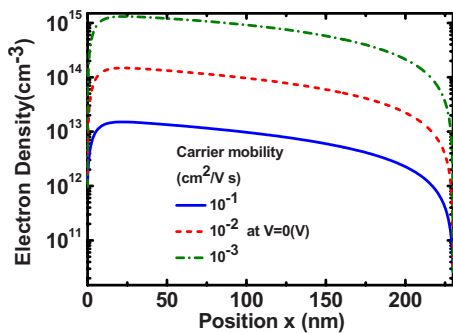


FIG. 18. (Color online) The electron density for various mobilities in the bulk with Schottky contact at short-circuit condition.

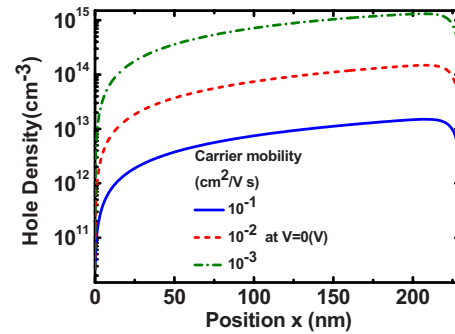


FIG. 19. (Color online) The electron density for various mobilities in the bulk with Schottky contact at short-circuit condition.

short-circuit current density  $J_{SC}$  for carrier mobility  $10^{-1}$   $\text{cm}^2/\text{V s}$  shown in Fig. 16 and are become a source of great loss. The electron current density at flat band condition for various mobilities is shown in Fig. 21. As the mobility increases, the photocarriers are collected quickly by both the right electrodes and the wrong electrodes (the right part of Fig. 21). The recombination distribution in flat band condition is shown in Fig. 22. As the mobility increases the photorecombination decreases, as the case of short-circuit condition in Fig. 17. The electron and hole carrier density distribution at flat band voltage are shown in Figs. 23 and 24, respectively. The distribution of the carrier density become more uniform compared with that at short-circuit voltage shown in Figs. 18 and 19 because there is no built-in voltage in flat band condition. The potential energy of short-circuit voltage and flat band voltage are shown in Figs. 25 and 26. The potential energy remains nearly straight at both conditions with different carrier mobilities due to the high injection barrier height.

The performance of BHJ solar cell depends on the mobility as well as the energy levels of the donor and acceptors.<sup>22-24</sup> The short-circuit current density is mostly determined by the acceptor band gap whereas the open-circuit voltage determined by the difference between the HOMO level of the donor and the LUMO level of the acceptor. It is generally accepted that in the optimal case there is an offset around 0.5 eV between the LUMO levels of the donor and acceptor for efficiency exciton dissociation, and the donor band gap is around 1.9 eV as a compromise between absorption and open-circuit voltage. The ideal efficiency is 10% under the assumption of unity external quantum efficiency

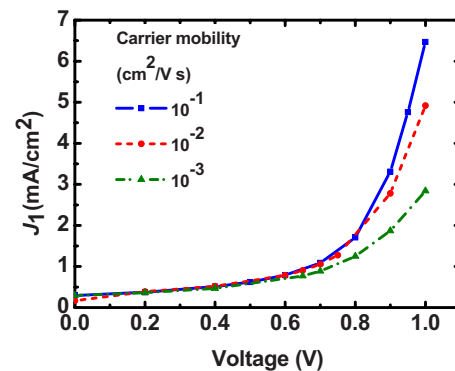


FIG. 20. (Color online)  $J_1$  as a function of applied voltage.



TABLE II. The current caused by photocarriers collected by the wrong electrodes at flat band with mobility from  $10^{-1}$  to  $10^{-3}$   $\text{cm}^2/\text{V s}$ .

$V=0.9$ V		
Mobility ( $\text{cm}^2/\text{V s}$ )	$J_1$ ( $\text{mA}/\text{cm}^2$ )	$J_2$ ( $\text{mA}/\text{cm}^2$ )
$10^{-1}$	3.31	3.31
$10^{-2}$	2.78	2.78
$10^{-3}$	1.87	1.88

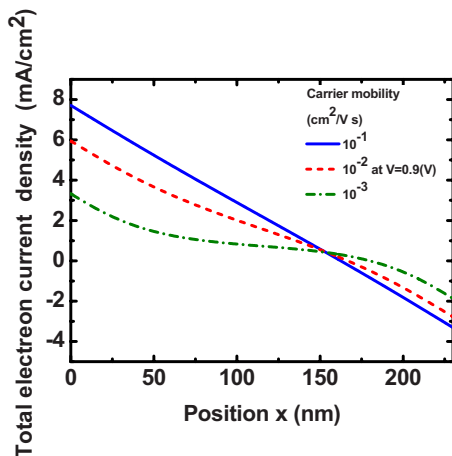


FIG. 21. (Color online) The electron density current distribution in the bulk with Schottky contact at flat band condition.

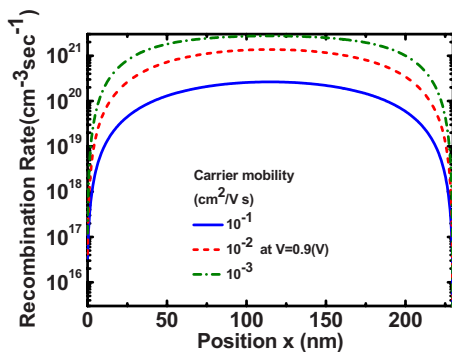


FIG. 22. (Color online) The recombination distribution for various mobilities with Schottky contact at flat band condition.

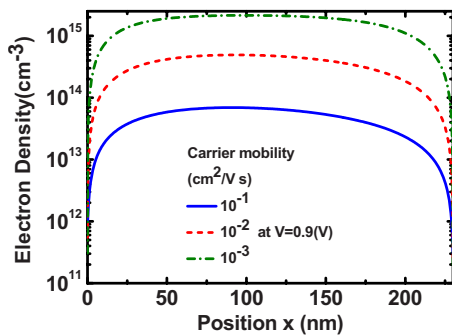


FIG. 23. (Color online) The electron density for various mobilities with Schottky contact at flat band condition.

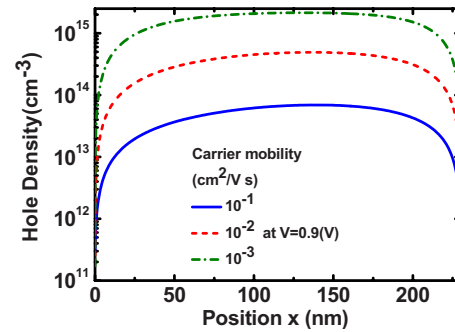


FIG. 24. (Color online) The hole density for various mobilities with Schottky contact at flat band condition.

for photons above band gap and fixed FF of 0.65.<sup>22</sup> Experimentally 6% PCE is observed due to recombination which reduces the quantum efficiency and the fill factor. The ideal levels are in fact quite close the most commonly used donor P3HT and acceptor PCBM (Ref. 24) which are leading in terms of efficiency despite of huge amount of new materials with other energy levels developed. In addition to energy levels mobility has been expected to be another major parameter to be optimized and recombination is thought to be possibly reduced with higher mobility. This work shows that the efficiency cannot be raised much by increasing mobility because of the dark carrier recombination. Increasing the energy barrier between metal and semiconductor will reduce the dark carrier recombination but sacrifice the light absorption. Our new finding in this work is therefore that for an optimal energy level it is impossible for improve the efficiency much beyond the current value by increasing the mobility because of the dark carrier recombination.

## VI. CONCLUSION

In conclusion we establish a numerical model to describe the microscopic properties and electrical characteristics of BHJ organic solar cells. By the analysis of the distribution of carrier density and recombination rate density it is shown that the PCE is limited by both the recombination with the photocarriers and recombination with dark carriers diffused from the metal electrode. The two recombination processes have opposite dependence on the carrier mobility. The best efficiency can be reached if one kind of carrier mobility is about  $10^{-2}$   $\text{cm}^2/\text{V s}$  and the other is within a tolerance range

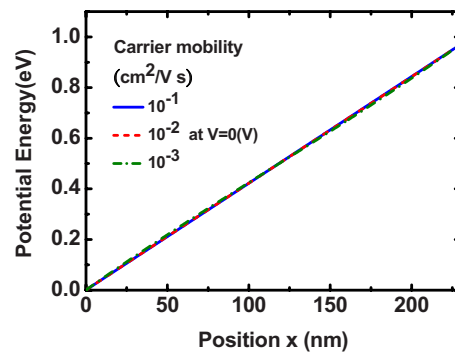


FIG. 25. (Color online) The potential energy as a function of position for various mobilities with Schottky contact at short-circuit condition.

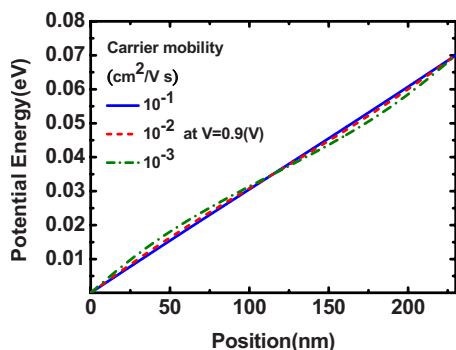


FIG. 26. (Color online) The potential energy as a function of position for various mobility with Schottky contact at flat band condition.

from  $10^{-1}$  to  $10^{-3}$   $\text{cm}^2/\text{V s}$ . The detrimental effect of dark carriers can only be avoided by a high energy barrier between the metal and the semiconductor. Unfortunately in practice with fixed semiconductor energy bands such barrier corresponds to a smaller metal work function difference a reduced open-circuit voltage. Our calculation predicts that with the inevitable dark carrier recombination for Ohmic contact there is not too much room for further efficiency improvement by simply tuning the material parameters such as the mobility and band gap. A more dramatic new device concept which simultaneously solves the dark carrier problem and the open-circuit problem is required to raise the organic solar cell efficiency far beyond the current value of around 6%.

## ACKNOWLEDGMENTS

This work is supported by the National Science Council of Taiwan under Grant Nos. NSC96-2120-M-007-007 and

NSC96-2112-M-009-036.

- <sup>1</sup>G. Li, V. Shrotriya, J. Huang, Y. Yao, T. Moriarty, K. Emery, and Y. Yang, *Nature Mater.* **4**, 864 (2005).
- <sup>2</sup>L. Ma, C. Y. Yang, X. Gong, K. Lee, and A. J. Heeger, *Adv. Funct. Mater.* **15**, 1617 (2005).
- <sup>3</sup>G. Li, V. Shrotriya, Y. Yao, and Y. Yang, *J. Appl. Phys.* **98**, 043704 (2005).
- <sup>4</sup>Y. Kim, S. A. Choulis, J. Nelson, D. D. C. Bradley, S. Cook, and J. R. Durrant, *J. Mater. Sci.* **40**, 6 (2005).
- <sup>5</sup>F. Padinger, R. S. Rittberger, and N. S. Sariciftci, *Adv. Funct. Mater.* **13**, 85 (2003).
- <sup>6</sup>J. Nakamura, K. Murata, and K. Takahashi, *Appl. Phys. Lett.* **87**, 132105 (2005).
- <sup>7</sup>P. W. M. Blom, V. D. Mihailetschi, L. J. A. Koster, and D. E. Markov, *Adv. Mater.* **19**, 1551 (2007).
- <sup>8</sup>M. Mandoc, L. Koster, and P. Blom, *Appl. Phys. Lett.* **90**, 133504 (2007).
- <sup>9</sup>L. Koster, E. Smits, V. Mihailetschi, and P. Blom, *Phys. Rev. B* **72**, 085205 (2005).
- <sup>10</sup>C. Deibel, A. Wagenpfahl, and V. Dyakonov, *Phys. Status Solidi (RRL)* **2**, 175 (2008).
- <sup>11</sup>T. Kirchartz, B. Pieters, K. Taretto, and U. Rau, *Phys. Rev. B* **80**, 035334 (2009).
- <sup>12</sup>C. Braun, *J. Chem. Phys.* **80**, 4157 (1984).
- <sup>13</sup>Y. X. Wang, S. R. Tseng, H. F. Meng, K. C. Lee, C. H. Liu, and S. F. Horng, *Appl. Phys. Lett.* **93**, 133501 (2008).
- <sup>14</sup>P. Langevin, *Ann. Chim. Phys.* **28**, 433 (1903).
- <sup>15</sup>U. Albrecht and H. Bassler, *Chem. Phys.* **199**, 207 (1995).
- <sup>16</sup>M. J. Tsai and H. F. Meng, *J. Appl. Phys.* **97**, 114502 (2005).
- <sup>17</sup>C. H. Chen and H. F. Meng, *Appl. Phys. Lett.* **86**, 201102 (2005).
- <sup>18</sup>P. S. Davids, I. H. Campbell, and D. L. Smith, *J. Appl. Phys.* **82**, 6319 (1997).
- <sup>19</sup>A. M. Goodman and A. Rose, *J. Appl. Phys.* **42**, 2823 (1971).
- <sup>20</sup>J. E. Parmer, A. C. Mayer, B. E. Hardin, S. Scully, M. D. McGehee, M. Heeney, and I. McCulloch, *Appl. Phys. Lett.* **92**, 113309 (2008).
- <sup>21</sup>L. J. A. Koster, V. D. Mihailetschi, and P. W. M. Blom, *Appl. Phys. Lett.* **88**, 052104 (2006).
- <sup>22</sup>M. Scharber, D. Muhlbacher, M. Koppe, P. Denk, C. Waldauf, A. Heeger, and C. Brabec, *Adv. Mater.* **18**, 789 (2006).
- <sup>23</sup>K. Coakley and M. McGehee, *Chem. Mater.* **16**, 4533 (2004).
- <sup>24</sup>L. Koster, V. Mihailetschi, and P. Blom, *Appl. Phys. Lett.* **88**, 093511 (2006).